Tech. J., vol. 40, pp. 197–212, 1961.
[3] A. A. M. Saleh, "Polarization-independent, multilayer dielectrics at oblique incidence," *Bell Syst. Tech. J.*, vol. 54, pp. 1027–1049, 1975.
[4] M. Born and E. Wolf, *Principles of Optics.* London, England: Pergamon, 1970, pp. 38–41.
[5] E. T. Harkless *et al.*, "WT4 millimeter waveguide system: Channelization," *Bell Syst. Tech. J.*, vol. 56, pp. 2089–2101, 1977.
[6] E. A. Marcatili, "Miter elbow for circular electric mode," in *Proc. Symp. on Quasi-Optics*, Brooklyn, NY: Polytechnic Press, 1964, pp. 535–543.

Cylindrical TE_{011}/TM_{111} Mode Control by Cavity Shaping

HERBERT L. THAL, JR. MEMBER, IEEE

***Abstract*—An appropriate modification of the shape of a cylindrical filter cavity has been used to separate the degenerate TM_{111} (doublet) modes while at the same time providing a slight increase in the already high unloaded Q of the desired TE_{011} mode. Experimental results of mode frequencies and unloaded Q's are tabulated for a family of shaped cavities. Two low-loss filters utilizing these cavities are discussed. The general correspondence between modes of spherical, cylindrical and rectangular cavities and waveguides is described in order to place the performance of intermediate shapes in perspective.**

I. Introduction

THE TE_{011} cylindrical cavity mode is potentially attractive for use in low-loss filters [1], [2] since it offers a higher unloaded Q than other modes having comparable cavity volumes, and it is easily tuned by a noncontacting, movable end wall. However, it is degenerate with a pair of TM_{111} modes which must be perturbed in some manner to make the TE_{011} mode usable. The required perturbation increases as the bandwidth of the filter increases; for multiplexer applications it is necessary to have the output cavity (at least) free of spurious modes over the entire multiplexed bandwidth since a weakly coupled resonance could introduce an absorption notch in one of the other channels even without producing a spurious transmission response. Previously described reactive or dissipative techniques degrade the TE_{011} Q in the process of controlling the TM_{111} mode whereas the approach covered in this paper yields a significant detuning of the TM_{111} resonance with a small increase in the TE_{011} Q as a by-product.

II. TM_{111} Mode Control

This method may be understood by relating the modes of a cylindrical cavity to those of a spherical cavity [3] as illustrated in Fig. 1. (General mode relationships are given in the Appendix.) The normalized parameter $Q\delta/\lambda_0$ is shown for each mode; δ is the skin depth and λ_0 is its resonant wavelength. The value of 0.641 for the TE_{011} mode is close to the maximum of 0.659 which occurs at a D/L of 1.00. Because of its symmetry the sphere has fewer different resonant frequencies but higher order degeneracies at each as indicated by the superscripts in parentheses. In general the spherical mode Q's are higher than the corresponding cylindrical ones. If the cavity were deformed from a cylindrical to a spherical shape, the resonances would move continuously from one family to the other as indicated schematically by the straight lines. Thus the figure suggests that there should be intermediate shapes which isolate the desired (cylindrical) TE_{011} mode from the degeneracies that exist in the cylindrical and spherical cases.

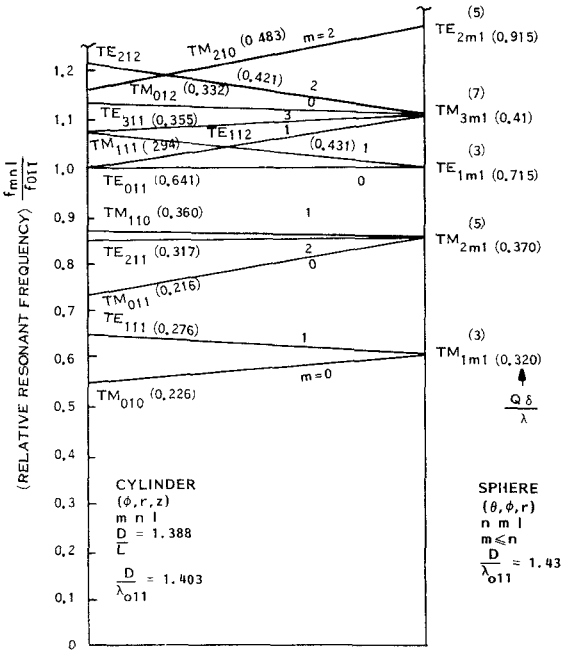

Fig. 1. Resonances of cylindrical and spherical cavities.

A cavity with chamfered ends as shown in Fig. 2 provides a mechanically convenient transitional shape which has been studied experimentally. Measurements

Manuscript received April 17, 1979; revised August 17, 1979.
The author is with Space Division, General Electric Company, Philadelphia, PA 19101.

0018-9480/79/1200-0982$00.75 ©1979 IEEE

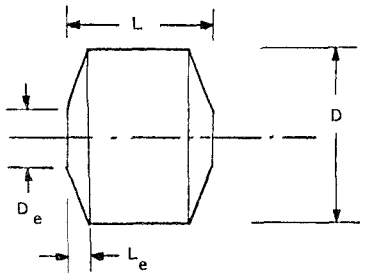

Fig. 2. Shaped cavity geometry.

SHAPE	CYLINDER	A	B	C	SPHERE	E	F	G
D (inches)	1.378	1.378	1.378	1.378	1.408*	1.430	1.430	1.430
L	0.993	1.097	1.142	1.213	- - -	1.186	1.135	1.109
D_e	0	0.520	0.520	0.520	- - -	0.800	0.800	0.800
L_e	0	0.110	0.165	0.250	- - -	0.315	0.315	0.315
f_o (TE_{011}) MHz	12009	11944	11936	11990	12009	11699	11861	11953
RELATIVE $\frac{Q\delta}{\lambda}$	1.000	1.053	1.077	1.042	1.115*	0.999	1.043	1.010

RELATIVE MODE FREQUENCIES

(CYLINDER NOTATION)								
$TE_{3,1}$	1.074*	1.0851	1.0900	1.0964	1.1067*	1.1021	1.1038	1.1046
$TE_{1,2}$	1.074*	1.0498	1.0408	1.0275	1.0000*	1.0356	1.0536	1.0633
TM_{111}	1.000*	1.0289	1.0445	1.0624	1.1067*	1.1137	1.1249	1.1308
$TE_{0,1}$	1.000	1.0000	1.0000	1.0000	1.0000	1.0000	1.0000	1.0000
TM_{110}	0.869*	0.8812	0.8817	- - -	0.8613*	-	0.8761	0.8730
$TE_{2,1}$	0.851*	0.8579	0.8605	0.8633	0.8613*	0.8668	0.8717	0.8743

* COMPUTED VALUE

Fig. 3. Measured characteristics of shaped cavities.

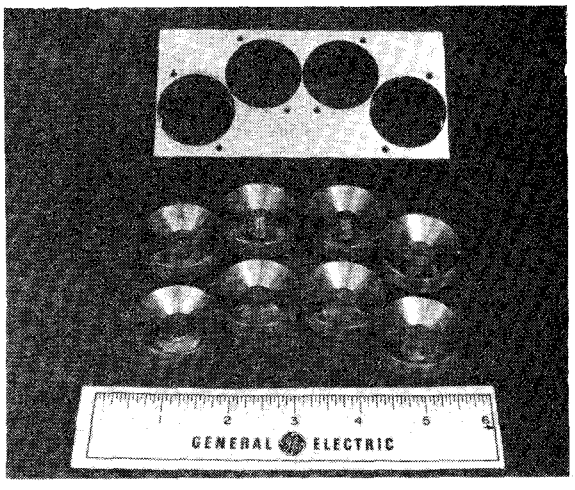

Fig. 4. Four-pole Chebyshev filter with shaped ends removed.

were taken over several half-power bandwidths using an automatic network analyzer and a small coupling aperture to minimize perturbations. These data were then computer processed to obtain best-fit values for the resonant frequency and the unloaded and external Q values. Shapes A, B, and C of Fig. 3 show the effect of increasing the depth of the conical end regions from zero (cylinder) towards an approximately spherical shape. The resonant frequencies shift in the manner indicated by Fig. 1. The Q_u values of the chamfered cavities fall between the cylindrical and the higher spherical values. Shapes E, F, and G of Fig. 3 comprise another family having a larger flat end and a deeper conical portion. These shapes have in general increased mode separation but slightly lower unloaded Q's. Chamfering could be used at one end only with correspondingly less effect if desirable for mechani-

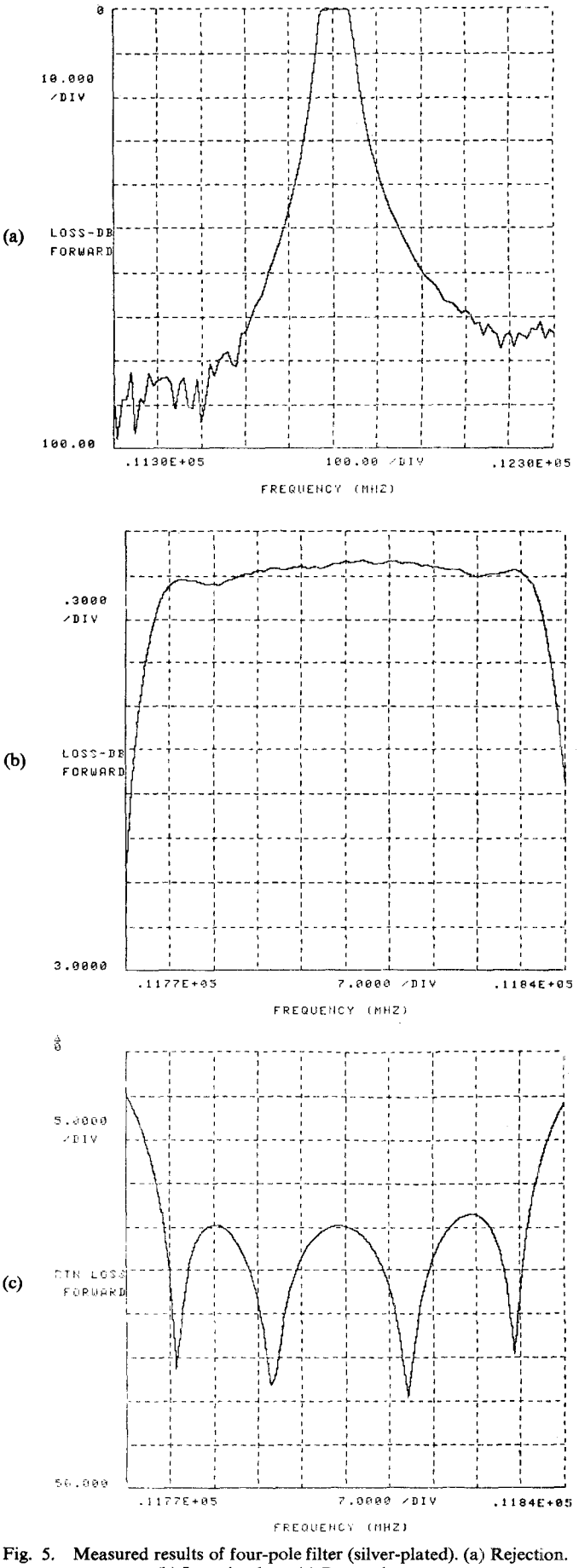

Fig. 5. Measured results of four-pole filter (silver-plated). (a) Rejection. (b) Insertion loss. (c) Return loss.

cal reasons, but no single-end configurations were measured.

III. Four-Pole Chebyshev Filter

Cavity shaping of this type has been used in filters having various side- and end-wall coupling arrangements which yield Chebyshev or elliptic responses. Fig. 4 shows an aluminum 12-GHz four-pole Chebyshev filter which utilizes cavity shape B. Coupling is provided by circular apertures in the sidewalls. Fig. 5(a) shows a wideband response of this filter (after silver-plating) taken on an automatic network analyzer, Fig. 5(b) shows the in-band transmission response, and Fig. 5(c), the return loss. The effective unloaded Q is in excess of 20000 based not only on the insertion loss of Fig. 5(b) but also on the complex values of all the scattering parameters [4]. Reducing the bandwidth should increase the Q towards the unperturbed value of 29700 projected from the measurements of Fig. 3.

IV. Six-Pole Elliptic Filter

A six-pole version having an elliptic response is shown in Fig. 6. The cavities are arranged in two tiers [2] with the input and output at the same end to allow for the one-to-six and two-to-five couplings required for this response. Cavities two and five utilize shape C; their axes are offset with a coupling aperture in the conical portions to provide an opposite sense to the one-to-six and three-to-four couplings. The other cavities are approximately shape F so that they are free of any spurious resonances within five percent of the design frequency. The uncoupled end of each cavity is movable to permit tuning.

Fig. 7(a) shows the rejection characteristic for a ± 5-percent frequency range (157 data points). The weakly excited TE_{112} resonances of cavities 2 and 5 cause a slight perturbation on the upper skirt but are not detectable in the return loss response. Fig. 7(b) gives an expanded view of the near-in portion (101 data points). Fig. 8 compares the measured and computed insertion loss based on a Q_u of 20000 and coupling values which best represent the experimental filter [4]. The measured insertion loss is less than the computed across the entire band for this value of Q_u.

V. TE_{211}/TE_{311} Mode Effects

The TE_{211} and TE_{311} modes which lie below and above the TE_{011} mode can lead to spurious transmission responses and perhaps even more importantly to contamination of the desired pass band. Consider a sidewall coupling arrangement shown schematically in Fig. 9. Energy coupled (magnetically) into the Nth cavity from the $(N-1)$th travels around the surface, reflecting from the symmetry plane and creating a standing-wave pattern which couples to the $(N+1)$th cavity in proportion to the magnetic field (squared) at the location of its coupling aperture. At the TE_{211} resonance the magnetic field has nulls at 45° and 135°; at the TE_{311} resonance the nulls are at 30°, 90°, and 150°. At the desired TE_{011} operating

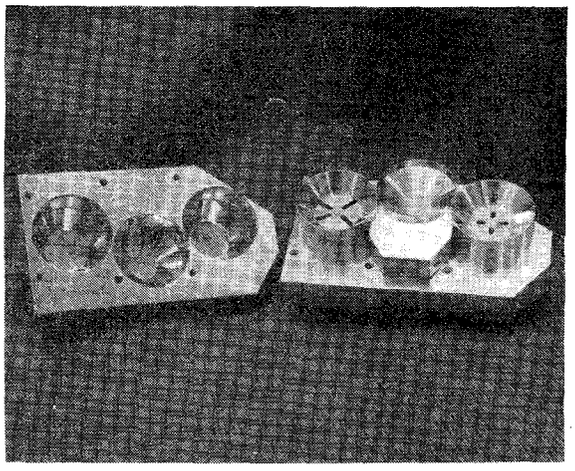

Fig. 6. Internal view of six-pole elliptic filter.

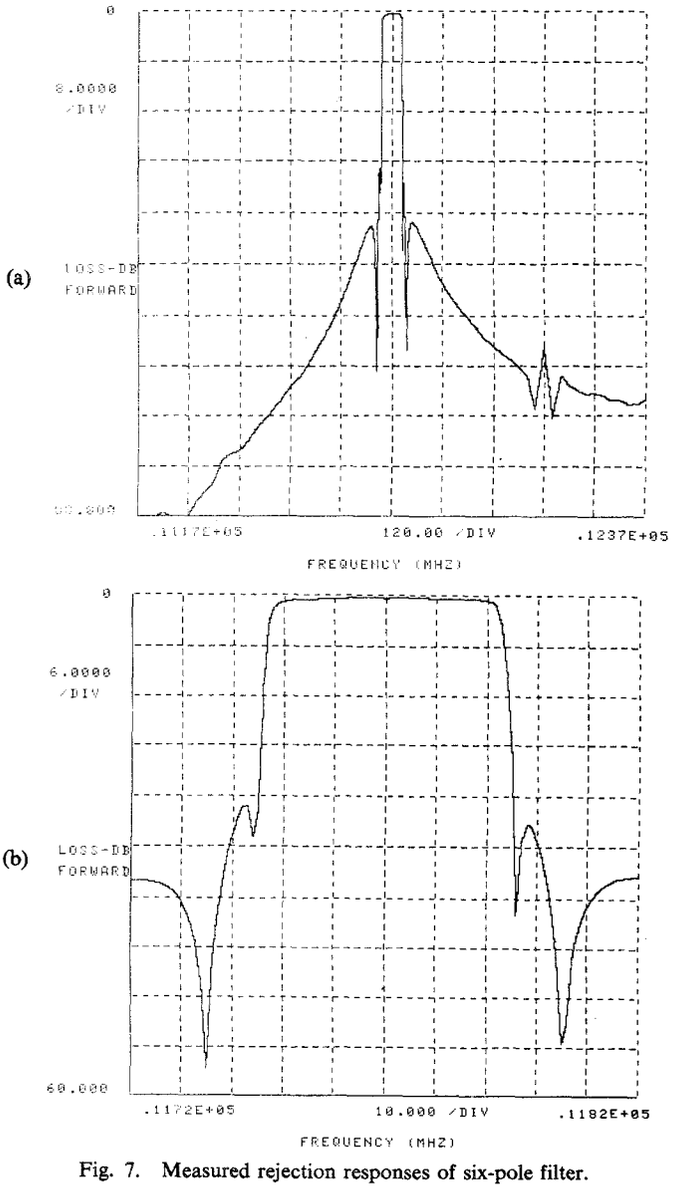

Fig. 7. Measured rejection responses of six-pole filter.

frequency the residual nonresonant TE_{211}/TE_{311} pattern has nulls at (intermediate) angles in the vicinity of 36° and 108°. Thus an angle of approximately 36° should be a

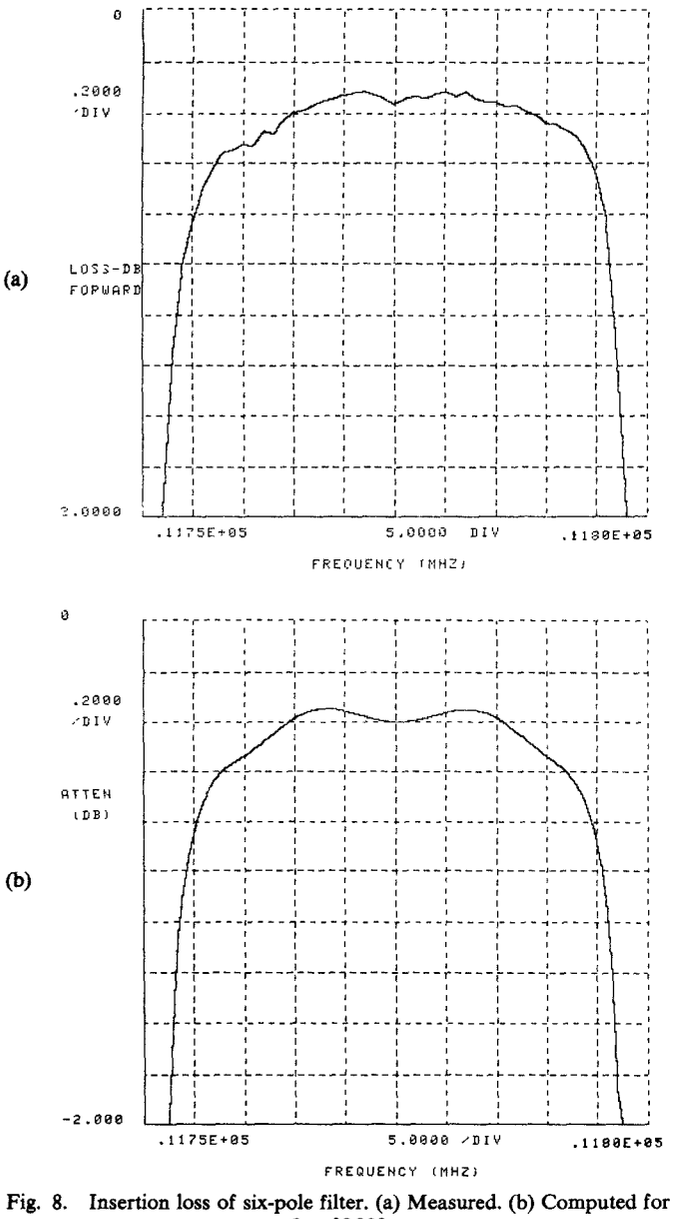

Fig. 8. Insertion loss of six-pole filter. (a) Measured. (b) Computed for $Q_u = 20000$.

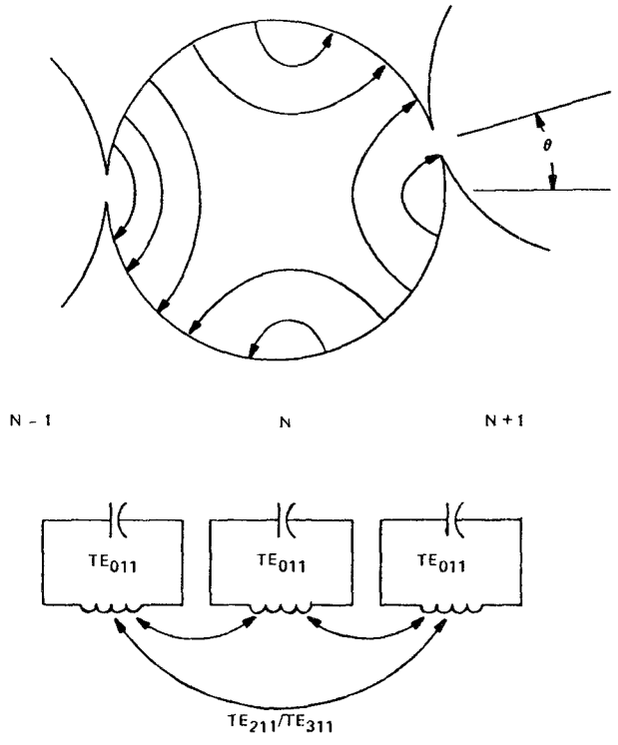

Fig. 9. Schematic of cavity geometry and equivalent circuit for TE_{211}/TE_{311} coupling mechanism.

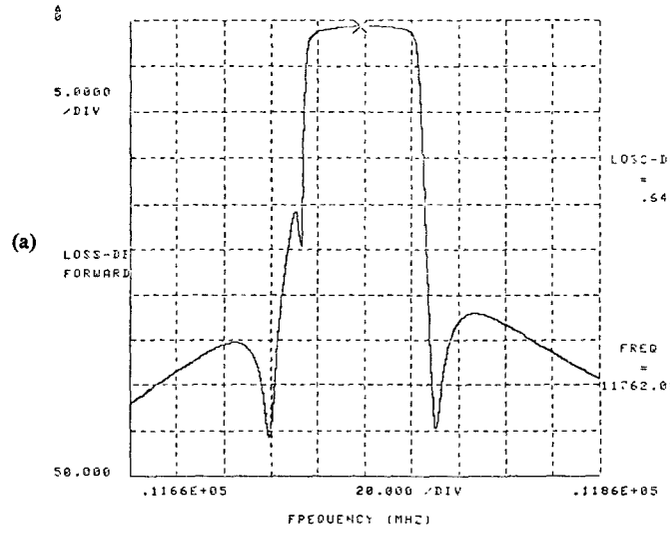

(b)

		Δf(MHz)		f(MHz)
0	1	42.80	1	11762.3
1	2	36.38	2	11761.1
2	3	22.92	3	11762.1
3	4	36.90	4	11762.1
4	5	22.92	5	11761.1
5	6	36.38	6	11762.3
6	7	42.80		
2	5	-16.64		
1	6	3.85		
1	3	-2.38		
4	6	-2.38		

Fig. 10. Effect of TE_{211}/TE_{311} contamination. (a) Measured response. (b) Equivalent (symmetrical) coupling values and resonant frequencies showing one-to-three and four-to-six terms.

good compromise for suppressing all three cases. Coupling of the desired TE_{011} modes is independent of this angle.

The six-pole filter shown in Fig. 6 has θ equal to 34.5°. A similar (unplated aluminum) filter using 20.6° gave the measured asymmetrical response of Fig. 10(a) which is accurately matched by a computed response using the coupling values of Fig. 10(b). The asymmetry is due to the 1–3 and 4–6 values which represent this nonresonant coupling mechanism; since they involve two apertures, they should increase as the square of the filter bandwidth (instead of linearly). Therefore, this effect becomes more critical as the bandwidth increases.

The same mechanism is involved with end-wall coupling, but multiple apertures may be used to advantage. The coupling is cumulative for the desired TE_{011} mode, but the multiple locations may be adjusted to yield cancellation for the undesired modes. Fig. 6 illustrates some configurations.

Appendix
Correspondence of Spherical, Cylindrical, and Square Cavity and Waveguide Modes

Since both the cylindrical and spherical cavities are symmetric about the z axis, corresponding modes must

TABLE I
CORRESPONDENCE OF CYLINDRICAL AND SPHERICAL CAVITY MODES

	CYLINDRICAL CAVITY (ϕ,r,z)	SPHERICAL CAVITY (θ,ϕ,r)
$m = 0$	TE_{0np}	TE_{p0n}
	TM_{0np}	$TM_{(p+1)0n}$
$m = 1$	TE_{1np}	TM_{p1n}, for $p = 1$ $TE_{(p-1)1n}$, for $p > 1$
	TM_{1np}	$TM_{(p+2)1n}$
$m \geq 2$	TE_{mnp}	$TM_{(p+m-1)mn}$
	TM_{mnp}	$TE_{(p+m)mn}$

TABLE II
CORRESPONDENCE OF CYLINDRICAL AND SQUARE WAVEGUIDE MODES

	CYLINDRICAL WAVEGUIDE (ϕ,r)	RECTANGULAR WAVEGUIDE (x,y)
$m = 0$	TE_{0n}	$TE_{(2n)0} + TE_{0(2n)}$
	TM_{0n}	$TM_{(2n-1)1} + TM_{1(2n-1)}$
EVEN $m \geq 2$	$TE_{(m-1)n}$	$TE_{(q-1)(k-1)}$ $TE_{(k-1)(q-1)}$
$q \equiv m/2$ $k \equiv 2n-1+q$	TE_{mn}	$TE_{(k-1)q} + TE_{q(k-1)}$ $TE_{k(q-1)} - TE_{(q-1)k}$
	$TM_{(m-1)n}$	TM_{qk} TM_{kq}
	TM_{mn}	$TM_{k(q+1)} + TM_{(q+1)k}$ $TM_{(k+1)q} - TM_{q(k+1)}$

have the same ϕ variations; that is in the notation of Fig. 1, the first cylinder index (m) must always be equal to the second sphere index (m). Within each m group comparison of the patterns and midplane symmetries leads by induction to the complete generalized set of Table I. Note that the radial indices (second cylinder and third sphere) are equal also. However, the first spherical index is a function of both the first and third cylindrical indices. Furthermore, the TE/TM notation is reversed in most cases since different surfaces are involved in defining the transverse fields.

The cylindrical resonances can in turn be related to square cavity resonances if the correspondence between circular and square waveguide modes is known by adding a third (length) subscript which is the same for both. Table II gives the correspondence for all modes (including doublets) and should be applicable to problems involving transitions, radiating apertures, cross section perturbations or numerical techniques in addition to resonant cavities. Note that all circular modes having an even value of m correspond to the sum or difference of two square modes (doublets); in particular, the low-loss circular TE_{01} mode is analogous to the sum of the square TE_{20} and TE_{02} modes. As another example, the two circular TM_{22} doublets correspond to the square mode sum $(TM_{42}+TM_{24})$ and to the difference $(TM_{51}-TM_{15})$. (For $n=1$ the two square modes in the sum have the same indices indicting a singlet instead of the sum of two doublets.)

ACKNOWLEDGMENT

The author wishes to acknowledge the contribution of G. Ditty to the design and testing of the experimental models.

REFERENCES

[1] G. L. Matthaei, L. Young, and E. M. T. Jones, *Microwave Filters, Impedance-matching Networks, and Coupling Structures*. New York: McGraw-Hill 1964, pp 921–934.

[2] A. E. Atia and A. E. Williams, "General TE_{011} mode waveguide bandpass filters," *IEEE Trans. Microwave Theory Tech.*, vol. MTT-24, pp 640–648, Oct. 1976.

[3] M. E. Currie, "The utilization of degenerate modes in a spherical cavity," *J. Appl. Phys.*, vol. 24, no. 8, pp 998–1003, Aug. 1953.

[4] H. L. Thal, "Computer-aided filter alignment and diagnosis," *IEEE Trans. Microwave Theory Tech.*, vol. MTT-26, pp 958–963, Dec. 1978.